Ion-Exchange Controls the Kinetics of Deswelling of Polyelectrolyte Microgels in Solutions of Oppositely Charged Surfactant

Peter Nilsson and Per Hansson*

Department of Pharmacy, Uppsala University, Box 580, S-75123 Uppsala, Sweden

Received: August 26, 2005; In Final Form: October 25, 2005

The kinetics of deswelling of sodium polyacrylate microgels (radius 30−140 μm) in aqueous solutions of dodecyltrimethylammonium bromide is investigated by means of micropipet-assisted light microscopy. The purpose of the study is to test a recent model (*J. Phys. Chem. B* **2003**, *107*, 9203) proposing that the rate of the volume change is controlled by the transport of surfactant from the solution to the gel core (ion exchange) via the surfactant-rich surface phase appearing in the gel during the volume transition. Equilibrium swelling characteristics of the gel network in surfactant-free solutions and with various amounts of surfactant present are presented and discussed with reference to related systems. A relationship between gel volume and degree of surfactant binding is determined and used in theoretical predictions of the deswelling kinetics. Experimental data for single gel beads observed during deswelling under conditions of forced convection are presented and compared with model calculations. It is demonstrated that the dependences of the kinetics on initial gel size, the surfactant concentration in the solution, and the liquid flow rate are well accounted for by the model. It is concluded that the deswelling rates of the studied gels are strongly influenced by the mass transport of surfactant between gel and solution (stagnant layer diffusion), but only to a minor extent by the transport through the surface phase. The results indicate that, during the volume transition, swelling equilibrium (network relaxation/transport of water) is established on a relatively short time scale and, therefore, can be treated as independent of the ion-exchange kinetics. Theoretical aspects of the kinetics and mechanisms of surfactant transport through the surface phase are discussed.

1. Introduction

The interaction between charged polymer networks and oppositely charged multivalent species is of great importance in nature. For instance, it plays a major role in the cellular secretion of many hormones and neurotransmitters[1] and has been suggested to be involved in the sorting of proteins in the Golgi and post-Golgi assemblies.[2,3] Secretory products are stored in secretory vesicles, often containing a charged proteoglycan network.[4] Recently, secretory vesicles have been recognized as prototypes for biomimetic drug delivery systems.[5,6] The release of the secretory vesicle contents to the extracellular space has been shown to involve an ion exchange[7] coupled to a volume expansion of the network.[1] The release kinetics has been suggested to be controlled by polymer network diffusion,[8] but the mechanisms involved are poorly understood. In general, for small networks (microgels), ion-exchange kinetics should be influenced by mass transport through the surrounding liquid layers. Furthermore, the distribution of the components in the microgels, depending in turn on the interactions involved, is expected to be of importance, as evident from recent studies of proteins[9] and self-assembling amphiphilic molecules[10,11] interacting with synthetic polyelectrolyte gels. The interaction, which is favorable from an electrostatic point of view, is very strong and typically reinforces a volume collapse of preswollen gels.[12−14] Importantly, the collapse starts at the exterior parts of the gel, and during the transition, there is a boundary between the dense surface phase and the swollen interior (core).[15,16] So far, the most detailed studies of surface phases have been made with alkyltrimethylammonium surfactants (C_nTA^+) binding to sodium polyacrylate (PA) gels.[10,13,17] In this case, the phases formed are structurally ordered, with globular or rodlike micelles ordered on cubic and hexagonal lattices, respectively,[17,18] resembling those formed by surfactants and oppositely charged non-cross-linked polyions.[19] During the major part of the volume collapse, the surface phase is very thin in comparison with the radius of the core. Nevertheless, the volume of the core, and thus the total gel volume, is markedly influenced by the surface phase. In a recent paper,[17] it was shown that the swelling of the core is reduced due to the additional work of deforming the network in the surface phase. The surface phase formed when $C_{16}TA^+$ is absorbed by PA gels was found to have rubber-like properties. The swelling of the partially collapsed gels could be accounted for theoretically by modeling the surface phase by using the theory of rubber elasticity.[17] Very recently, it was demonstrated that certain properties of the surface phase, such as thermodynamic stability and elasticity, influence the deswelling kinetics of poly(styrenesulfonate) microgels in solutions of cationic surfactants.[11]

Interestingly, surface phases seem to play a similar role when proteins bind to weakly cross-linked gels.[9,20−22] However, for proteins and other macromolecules, a dense surface phase may represent an important diffusion barrier. For surfactants, this is less obvious due to the transport mediated by monomers. In the present paper, we demonstrate that the binding of $C_{12}TA^+$ to small PA gels is dominated by "stagnant layer" diffusion. This was suggested in a previous study on the same system, where a theoretical model of the deswelling kinetics was presented.[10] The model describes the transport of surfactant from

* Corresponding author. E-mail: per.hansson@farmaci.uu.se.

10.1021/jp054835d CCC: $30.25
Published on Web 11/23/2005

the bulk solution to the boundary between the surface phase and core, where the growth of the former takes place. However, the experiments in that study were performed under rather primitive conditions with gels placed in unstirred solutions at the bottom of a beaker. The results that will be presented here are obtained with an improved technique, where gels are manipulated by using micropipets.[11,23] The experimental setup permits us to position single gel beads in a surfactant solution with a controlled liquid flow rate. Various parameters included in the model will be tested systematically. We also present equilibrium swelling data for various degrees of surfactant binding to the gels, serving as a basis for calculations of theoretical deswelling curves used in the evaluation of the kinetic model.

2. Experimental Section

2.1. Materials. Dodecyltrimethylammonium bromide (C_{12}-TAB) (99%), acrylic acid (99%), bis(2-ethylhexyl) phthalate 99%, and poly(vinyl chloride) (PVC) from Aldrich, ammonium persulfate for electrophoresis, *N*,*N*′-methylenebisacrylamide, and *N*,*N*,*N*′,*N*′-tetramethylethylenediamine (TEMED) (99%) from Sigma, sodium hydroxide (NaOH) from Eka Chemicals, sodium chloride (NaCl) (Baker analyzed) from Tamro, sodium bromide (NaBr) from Kebo, potassium chloride (KCl) and tetrahydrofuran p.a. (THF) from Merck, and acetone from Riedel−de Haën were all used as received. Solutions were prepared by using high-quality Millipore water.

2.2. Preparation of Gels. Submillimeter gels were prepared by using the inverse suspension polymerization method (1% cross-linker) described elsewhere[10] with the following modifications: 1 mL of reaction mixture was injected into the oil and equilibrated for 5 min, after which 100 μL of ammonium persulfate solution (radical initiator) was added. The reaction was then performed at 70 °C for 30 min. The gels were washed repeatedly with pure water and acetone, discarding gels smaller than approximately 50 μm by filtration (filter funnel P2). The gels were then hand-sieved, and the fraction larger than 500 μm was discarded. Note that gel sizes will be smaller in 10.5 mM NaBr than in pure water.

Macroscopic gels were prepared as described elsewhere.[10] To get smaller gels (allowing for shorter equilibrium times), capillary tubes (r = 0.75 mm) were used. The cross-linker concentration was, as for the microgels, set to 1%.

2.3. Micromanipulation and Light Microscopy. Single gels were studied by using a light microscope (Olympus BX-51) equipped with a micromanipulator (Narishige ONM-1). All micropipets were pulled and polished by using a Narishige PC-10 puller and a MF-9 microforge. Unless stated otherwise, the gels were in contact with a bulk solution containing 10 mM NaBr and small amounts of NaOH (to ensure pH > 9 and thereby a fully charged network).

A small sample of gels was allowed to equilibrate in a Petri dish at given conditions until no change in gel size could be measured. After equilibration, a gel of suitable size was chosen and picked up with the micromanipulator by suction, using an IM-5A injector. A larger pipet (the flow pipet), connected to a peristaltic pump (Pharmacia Fine Chemicals model P-1), was placed under the microscope. The gel was positioned, centered inside the flow pipet (see Figure 1), and the bulk solution was recirculated. The solution being pumped through the flow pipet was then switched to one containing C_{12}TAB (0.5−1.0 mM), and digital images were captured and stored every 15 s by using an Olympus DP-50 digital camera. The images were analyzed with respect to gel size by using the Olympus DP-Soft software.

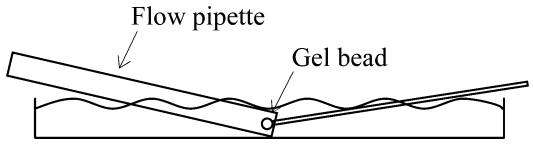

Figure 1. Schematic representation of the experimental setup. A single gel bead is immersed in the bulk solution and held in place in the center of the flow pipet. The pipets and the container are not drawn to scale.

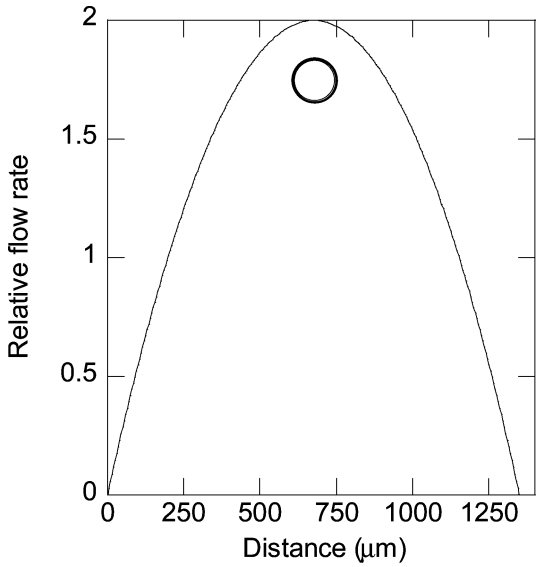

Figure 2. Relative flow rate (1 corresponds to the average flow rate in the pipet) at different distances from the pipet wall, assuming laminar flow. Also shown is a typical gel (R_0 = 70 μm) with a stagnant layer (grey).

For each image, the projected gel area was measured and recalculated to gel volume (V) assuming spherical gels.

The liquid velocity was calculated from the measured volume flow. For laminar flow, v in the center is equal to twice the average velocity in a pipe.[24] Figure 2 shows the relative flow in different parts of the pipet (with no gel present). A gel of typical size with a stagnant layer has been drawn for reference. Because a gel is considerably smaller than the dimension of the pipet, its presence gives rise to only a small perturbation of the velocity profile. Furthermore, the velocity where the gel is positioned changes little over distances equal to the stagnant layer thickness; see below. Therefore, in all calculations, v will be put equal to twice the average velocity.

2.4. Gel Swelling in Solutions of a Simple Electrolyte. Data underlying the construction of the pure network equation of state were obtained in the following way: Macrogels (dry weight approximately 50 mg) were placed in surfactant-free solutions of 500 mL of 70 mM NaBr pH 10 and allowed to equilibrate for at least 2 days. The electrolyte concentration was then lowered by dilution in a stepwise fashion down to 3 mM. For each concentration, the gel was allowed to equilibrate for 24 h, after which the gel weight was measured.

2.5. Swelling/Binding Isotherms in Surfactant Solutions. Macrogels were allowed to equilibrate for several weeks in C_{12}-TAB solutions of 10 mM NaBr, pH 10. The C_{12}TAB concentration was chosen with regard to the gel weight and the solution volume to achieve a surfactant/polymer ratio (β) in the range 0−0.9. V/V_0 and β were determined by weighing the equilibrated gels and measuring the bulk C_{12}TAB concentration by using a surfactant-active electrode. The surfactant-free gel (β = 0) was freeze-dried so that the volume per mole of polymer (v_0) could be calculated, and by relating that to the fully collapsed high-β gels, the corresponding value for collapsed gel was determined.

2.6. Gel Collapse in Bulk Solutions. To find the C_{12}TAB concentration at which PA gels collapse, macroscopic gels ($V_0 \approx 0.1$ mL) were placed in solutions ranging from 0.35 to 1.0 mM C_{12}TAB, 10 mM NaBr, pH 10. The volume of the solution was chosen so that the surfactant concentration would change less than 1% even if the entire gel collapsed. The gels were allowed to equilibrate for one year and then evaluated visually and characterized as swollen, collapsed, or partially collapsed.

2.7. Surfactant-Sensitive Electrode. C_{12}TAB concentrations were measured by a potentiometric method[25,26] utilizing a surfactant-sensitive electrode with a PVC membrane without charged carrier complex. The following cell was used: reference electrode (kalomel)|saturated KCl solution|1 M NH_4Cl agar bridge|reference solution (C_{12}TAB 10 mM, NaCl 10 mM)|PVC membrane|sample solution (C_{12}TAB $1 \times 10^{-5} - 3 \times 10^{-3}$ M, NaCl 10 mM)|1 M NH_4Cl agar bridge|saturated KCl solution|reference electrode (calomel). The PVC membrane was made from (by weight) 5.2% PVC, 17.0% bis(2-ethylhexyl)-phthalate and 77.8% THF. The electromotive force was measured with a Keithley 177 microvolt digital multimeter (DMM) and a Fluke 25 multimeter connected in series.

3. Theory

3.1. Swelling Equilibrium. The volume V of a core/skin gel relative to the volume V_0 prior to surfactant binding can be written:[17]

$$\frac{V}{V_0} = \frac{\upsilon_{core}}{\upsilon_0} - \left(\frac{\upsilon_{core} - \upsilon_{skin}}{\upsilon_0}\right)\beta' \qquad (1)$$

where υ_{core} is the volume per polyion charged group in the core, υ_{skin} is the corresponding quantity for the surface phase, and β' is the fraction of polymer present in the surface phase. The equilibrium swelling of the core can be calculated from:[17]

$$\Delta\pi_{ion} + \pi_{net} + \pi_{skin} = 0 \qquad (2)$$

The first term on the left-hand side is the osmotic pressure difference between the core and the solution due to the difference in ion activity. In the present work, this contribution will be estimated from numerical solutions of the Poisson−Boltzmann equation by using the cell model, as described in Appendix 1. The second term in eq 2 is the contribution to the osmotic pressure in the core due to the deformation of the core network, including the rubber elasticity and the free energy of mixing the polymer chains and water. Existing theoretical models of rubber elasticity, in general, fail to provide us with quantitatively correct predictions of polyelectrolyte gel swelling. However, because our objective is to demonstrate the importance of the surface phase, not the elasticity of pure networks, we need only an accurate functional relationship between π_{net} and υ_{core}, valid under the range of core network deformation ratios encountered here. Here, we shall use the method by Ricka and Tanaka[27] to extract out π_{net} from experimental data for gels in equilibrium with solutions of a simple electrolyte by subtracting the contribution from $\Delta\pi_{ion}$.[17] Note that, in surfactant-free solutions, where no surface phase is formed, π_{net} must be equal to $-\Delta\pi_{ion}$ for all values of υ_{core}.

The last term in eq 2 is the contribution to the osmotic pressure in the core due to the presence of the deformed surface phase. It can be calculated from:[17]

$$\pi_{skin} = -\left(\frac{\beta'}{1-\beta'}\right)\left(\frac{2RT}{3p{\upsilon_{skin}}^{2/3}{\upsilon_{core}}^{1/3}}\right)\left(1 - \left(\frac{\upsilon_{skin}}{\upsilon_{core}}\right)^2\right) \qquad (3)$$

where p is a material constant depending on the network structure.[28,29]

3.2. Deswelling Kinetics. The model we will employ was derived earlier.[10] A gel undergoing volume collapse is considered to consist of a swollen core network free from micelles and a collapsed surface phase (skin) containing micelles (complex salt). The gel is surrounded by a "stagnant" liquid layer, a construct used to describe the mass transfer between gel and bulk solution.[24]

According to the model, the surface phase starts to form when the surfactant concentration in the gel reaches a critical concentration. The existence of such a concentration, corresponding to the critical association concentration (cac) in the solution in equilibrium with the gel, was proved earlier.[14] The time to reach that concentration is denoted the lag time. The binding of surfactant during the lag period is described as a regular ion exchange controlled by stagnant layer diffusion.[30] The ion exchange proceeds during the deswelling as the surface phase grows. To model the surfactant uptake and the deswelling, the following assumptions are made:

1. The gel volume is constant during the lag period.
2. Micelles form when the average concentration of surfactant in the gel exceeds a critical concentration.
3. The formation of the surface phase and the onset of deswelling coincide with the appearance of micelles in the gel.
4. Local equilibrium is maintained at the skin/core interface.
5. The transport of surfactant from the bulk solution to the core is the process controlling the rate of deswelling.
6. Steady-state transport of surfactant is maintained during deswelling.
7. The volume of the gel, at any time during deswelling, is the same as it would be if the gel contained the same amount of surfactant at equilibrium.
8. The transport of surfactant from the bulk to the gel can be described by using "stagnant layers", despite the fact that the gel boundary moves as the gel deswells.

Assumptions 5 and 7 imply that the transport of surfactant and the gel swelling are treated as independent events. The rate of binding of surfactant, at any time, is then given by:[10]

$$\frac{d\beta}{dt} = \frac{3\upsilon_0 r_1 D(C_2 - cac)}{{R_0}^3\left(\frac{2}{2+Sh} + \left\{\frac{r_1}{r_0} - 1\right\}\frac{D}{P}\right)} \qquad (4)$$

β is the number of surfactant molecules per polyion charge in the gel, r_0 and r_1 are the core and gel radii at any given time, R_0 is the initial gel radius, υ_0 is the volume per mole of polyion charges in the gel prior to deswelling, C_2 is the surfactant concentration in the bulk, Sh is the Sherwood number describing the stagnant layer thickness (see Appendix 2), D is the effective diffusion coefficient in the stagnant layer, and P is the permeability of the surface phase to the surfactant (see below). The time for a gel to reach a shrunken state (β, r_1) can be calculated from the integrated form of eq 4:[10]

$$t = \frac{{R_0}^3}{3\upsilon_0 D(C_2 - cac)}\int_0^{\beta}\left(\frac{2}{2+Sh} + \left\{\frac{r_1}{r_0} - 1\right\}\frac{D}{P}\right)\frac{1}{r_1}\,d\beta \qquad (5)$$

The integral in eq 5 can be calculated from any data providing a relationship between the gel dimensions (r_0, r_1) and β, such as the equilibrium model described above or, under appropriate conditions, an experimental swelling isotherm.

Strictly, a permeability P can only be defined when there is a fixed chemical potential difference over the surface phase.

To describe the steady-state transport through the surface phase, we use the generalized form of Fick's first law,[31] which for diffusion through a spherical surface at a distance r from the center can be written:

$$\frac{dn}{dt} = -\frac{4\pi r^2 D_I C(r)}{RT} \times \frac{d\mu(r)}{dr} \quad (6)$$

where $C(r)$ is the local concentration of surfactant, $d\mu(r)/dr$ is the gradient in chemical potential, and D_I is the diffusion constant in the surface phase. The steady-state transport through the surface phase is obtained from an integration of eq 6 between r_0, where the chemical potential is μ_0 and r_1 (μ_1), noting that the flux dn/dt is constant and equal everywhere:

$$\frac{dn}{dt}\int_{r_0}^{r_1}\frac{dr}{r^2} = \frac{dn}{dt}\left(\frac{1}{r_0} - \frac{1}{r_1}\right) = -\frac{4\pi}{RT}\int_{\mu_0}^{\mu_1} D_I C(r)\, d\mu(r) \quad (7)$$

Because the rate of binding to the gel $d\beta/dt = (dn/dt)3v_0/4\pi R_0^3$, eq 7 can be rearranged to give:

$$\frac{d\beta}{dt} = \frac{3v_0 r_0 r_1}{R_0^3(r_1 - r_0)RT}\int_{\mu_0}^{\mu_1} D_I C(r)\, d\mu(r) \quad (8)$$

In the general case, both D_I and C are functions of r. However, for the special case of a surface phase containing closely packed micelles, with small variations of the surfactant concentration in the phase, D_I and C can be approximated as constants. This gives:

$$\frac{d\beta}{dt} \approx \frac{3v_0 r_0 r_1 D_I C(\mu_1 - \mu_0)}{R_0^3(r_1 - r_0)RT} = \frac{3v_0 r_0 r_1 D_I C \ln(C_1/\mathrm{cac})}{R_0^3(r_1 - r_0)} \quad (9)$$

where C_1 is the surfactant concentration at r_1, the interface between the surface phase and the surrounding solution.

The last equality follows from the condition of local equilibrium across the interfaces on each side of the surface phase, where:

$$\mu_1 = \mu^{0,w} + RT \ln C_1 \quad (10a)$$

$$\mu_0 = \mu^{0,w} + RT \ln \mathrm{cac} \quad (10b)$$

$\mu^{0,w}$ is the standard chemical potential of a surfactant molecule in water. Equation 9 can be used directly instead of eq 4 when stagnant layer diffusion is unimportant. In the general case, C_1 can be obtained from numerical solutions to the equation:

$$C_1 = C_2 - \frac{r_0 C D_I \ln(C_1/\mathrm{cac})}{(r_1 - r_0)(1 + Sh/2)D} \quad (11)$$

which derives from the steady-state condition that the surfactant flux is the same in the surface phase and the stagnant layer:

$$\frac{4\pi r_0 r_1 C D_I \ln(C_1/\mathrm{cac})}{r_1 - r_0} = 4\pi r_1(1 + Sh/2)D(C_2 - C_1) \quad (12)$$

The expressions on the left- and the right-hand side, respectively, describes the flux in the surface phase and the stagnant layer.[10]

In descriptions of membrane transport, it is common to write $P = KD_I$, where K is an equilibrium constant describing the partitioning of the diffusing species between membrane and solution.[32] The interpretation derives from Fick's first law for the case of diffusing species forming an ideal solution in the membrane, obviously not the case for the surface phase. However, for a fixed chemical potential difference over the surface phase, the rate eq 9 can be written:[10]

$$\frac{d\beta}{dt} = \frac{3v_0 r_0 r_1 P(C_1 - \mathrm{cac})}{R_0^3(r_1 - r_0)} \quad (13)$$

Comparison of eq 13 with eq 11 shows that P can be interpreted as a *conditional* permeability dependent on C_1:

$$P \approx \frac{D_I C \ln(C_1/\mathrm{cac})}{C_1 - \mathrm{cac}} \quad (14)$$

In the limit as C_1 goes to cac, the right-hand side of eq 14 becomes equal to $D_I C/C_1$. Because C/C_1 can be interpreted as a partition coefficient, the behavior resembles transport through a membrane: $P = D_I K$.

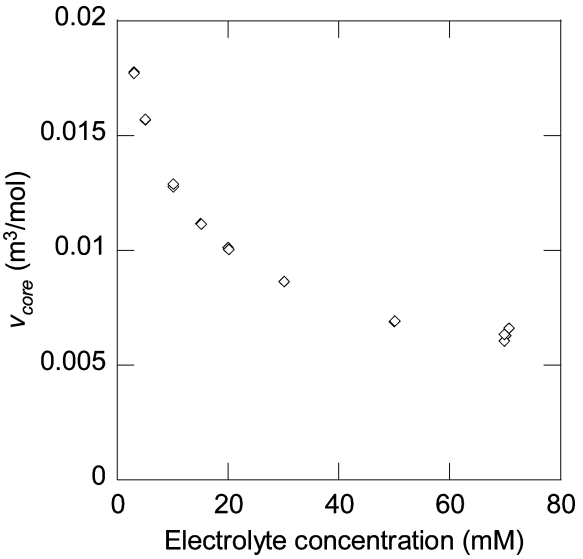

Figure 3. Deformation ratio (v_{core}) as a function of electrolyte concentration

4. Results and Discussion

The outline of this part of the paper is the following: In Sections 4.1−4.3 we investigate the equilibrium swelling of PA gels in the absence and presence of C_{12}TAB. The results are presented in terms of an "equation of state" for the core network, a binding isotherm, and a swelling isotherm, and analyzed by using eqs 1− 3. In Section 4.4, we describe how the equilibrium data are used in the kinetic analysis and motivate the choice of experimental conditions, in Section 4.5, we look at the nonvaried parameters in the kinetic model, and in Section 4.6, we test the model against experimental data. We then proceed to a discussion of the lag time in Section 4.7, followed by an analysis of the surfactant transport through the surface phase in Section 4.8. The influence of sodium ion diffusion is discussed in 4.9, and the relation between cac and volume transition in Section 4.10. Finally, in Section 4.11, we consider the kinetics of swelling in the light of our results.

4.1. Expressions for π_{net} and $\Delta\pi_{ion}$. To obtain a relationship between π_{net} and v_{core}, gels were placed in solutions of different electrolyte concentration (free from surfactant), and the gel volume (and thereby v_{core}) was determined at swelling equilibrium (Figure 3). For each v_{core}, we calculated $\Delta\pi_{ion}$ from the PB-cell model. Because $\pi_{skin} = 0$, we obtained π_{net} as a function of v_{core}, simply by putting $\pi_{net} = -\Delta\pi_{ion}$. The result is presented

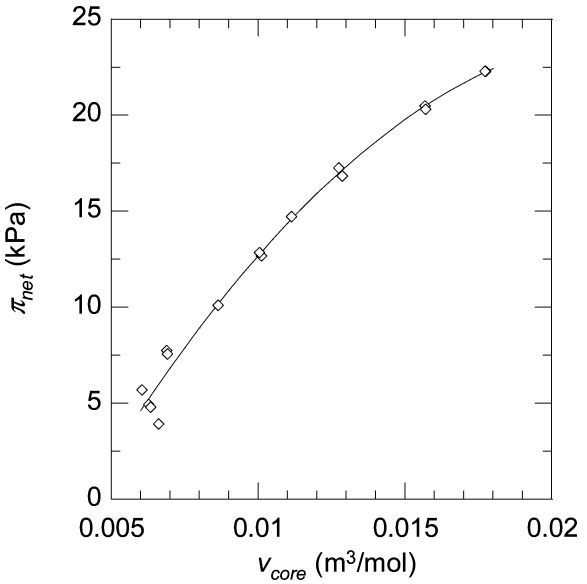

Figure 4. Osmotic pressure from the deformation of the gel network (π_{net}) as a function of the deformation ratio (v_{core}). The line is the result of a polynomial fit; eq 15.

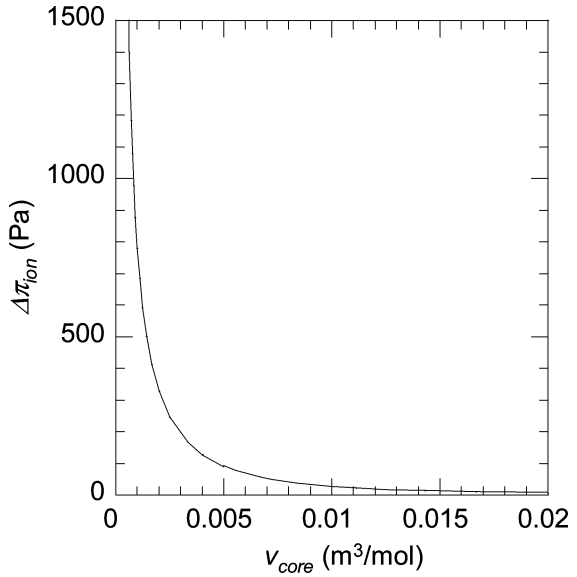

Figure 5. Osmotic swelling pressure from the ion activity ($\Delta\pi_{ion}$) in the gel as a function of the deformation ratio (v_{core}) at 10.5 mM salt; eqs 16a and b.

in Figure 4. The data are described well by a second-order polynomial (the line in Figure 4):

$$\pi_{net} = -11.5 - 3.08 \times 10^3 v_{core} + 6.67 \times 10^4 (v_{core})^2 \quad (15)$$

Equation 15 gives the pressure in units of *Pa* when v_{core} is expressed as m^3/mol. It can be considered as the "equation of state" for the uncharged backbone of the network. To obtain a complete functional description of the charged core network, we have also calculated, by using the PB-cell model, $\Delta\pi_{ion}$ as a function of v_{core} for gels in contact with a 10.5 mM salt solution. The results are described well by the following two equations and graphically presented in Figure 5.

$$\Delta\pi_{ion} = -52.4 + 0.706 {v_{core}}^{-1} + 1.25 \times 10^{-4} {v_{core}}^{-2} \qquad v_{core} \le 3.4 \times 10^{-4}\ \text{m}^3/\text{mol} \quad (16a)$$

$$\Delta\pi_{ion} = -16.2 + 0.357 {v_{core}}^{-1} + 8.94 \times 10^{-4} {v_{core}}^{-2} \qquad v_{core} \ge 3.4 \times 10^{-4}\ \text{m}^3/\text{mol} \quad (16b)$$

Again, the pressure is obtained in *Pa* units. In the next section, we use eqs 15 and 16 to analyze the effect of the surface phase on the swelling of PA gels in C_{12}TAB solutions. When used in combination, these equations give a good description of the swelling in the range encountered in the present study.

4.2. Relation Between Volume Transition and Binding Isotherm. Swelling data for PA gels in C_{12}TAB solutions are presented in Figure 6, where V/V_0 is given as a function of surfactant concentration. All solutions contained 10 mM NaBr and small amounts of NaOH (pH = 10). The plot shows data from two different experiments: In one (crosses), short cylinder-shaped gels were placed in large volumes of solution, where the absorption by the gels did not change the surfactant concentration to any appreciable extent. As can be seen, all gels collapsed when the concentration was $\ge$0.375 mM. In the collapsed state, the volume ($V/V_0 \approx 0.04$) was independent of surfactant concentration in the solution, and all gels seemed to have a homogeneous composition (single phase). At 0.350 mM, the gel volume was somewhat smaller than in the surfactant-free reference solution, but no surface phase could be detected.

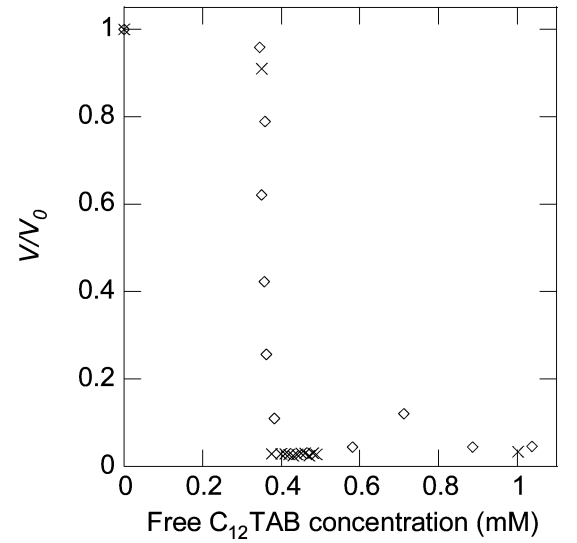

Figure 6. Relative gel volume as a function of free C_{12}TAB concentration for gels in (a) excess amounts of solution of constant concentration (crosses) and (b) solutions with limited amounts but high concentration of C_{12}TAB (diamonds). The former shows at which concentration the volume transition takes place, the latter the free concentration in equilibrium with (partially) collapsed gels.

The results show that a volume transition takes place in a very narrow range of surfactant concentrations. In principle, by including more data points in the critical range, it might be possible to decide if the transition is continuous or not. However, in practice, this is difficult, as the time for the gels to collapse approaches infinity near the cac due to the very small difference in the surfactant chemical potential between gel and solution.[10] For the gel at 0.375 mM, it took several days to reach the fully collapsed state. Because the gel at 0.350 mM had not collapsed after one year, its equilibrium state appears to be swollen.

In the second type of experiment, cylinder shaped gels ($V_0 \approx 1$ mL) were placed in solutions containing limited amounts of surfactant, not sufficient to collapse the whole gel, but with initial concentrations well above the cac. This allowed us to determine the concentration of surfactant in equilibrium with gels captured at intermediate stages of deswelling. The result is presented in Figure 6 (diamonds) as a plot of V/V_0 against

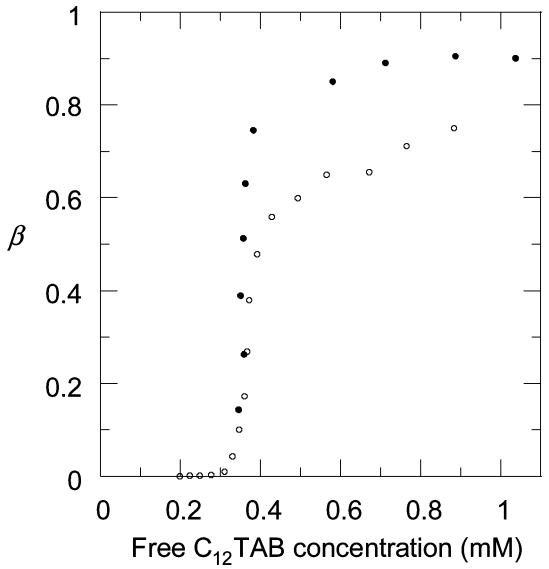

Figure 7. Binding isotherm for C_{12}TAB and cross-linked PA (filled) and linear, non-cross-linked PA (open). For cross-linked PA, the surfactant concentration is roughly constant at 0.36 mM until $\beta > 0.8$, after which it rises steeply. At $\beta = 0.9$, the binding of surfactant stops, and additional surfactant only increases the free concentration.

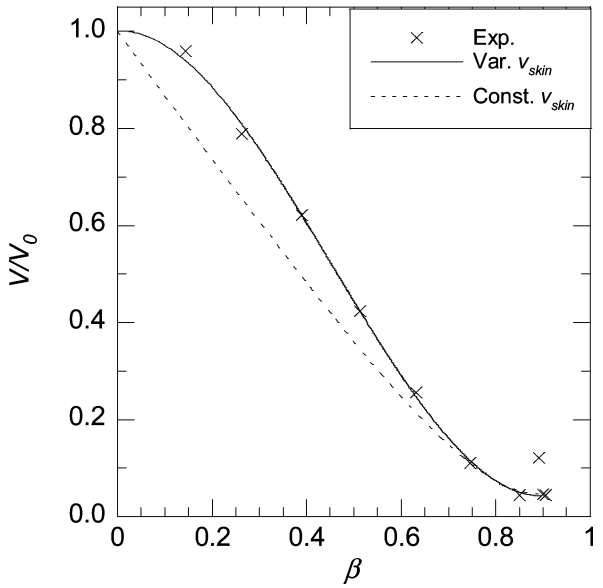

Figure 8. Swelling isotherm relating V/V_0 to β. Experimental values (crosses) and theoretical line with variable (solid line) and constant υ_{skin} (dotted line). The sigmoid shape can only be described correctly by allowing an initially higher υ_{skin}.

the concentration of surfactant remaining in the solution, and in Figure 7 as a binding isotherm. An examination showed that all gels in the interval $0.2 < \beta < 0.8$ had a core/shell structure. The major volume change can, therefore, be described as a gradual conversion of the swollen, micelle-free core into the collapsed surface phase.[13] The same phenomenon has been observed and studied in detail for PA/C_{16}TAB and PA/C_{16}TAC,[17] but was not recognized in an earlier paper devoted to the present system.[14] As can be seen in Figures 6 and 7, the concentration in the solution remains constant (within experimental error) during the course of the volume transition, and is equal to the transition concentration seen in the first experiment. Because the free concentration can be considered as equal to the activity of the surfactant, the growth of the surface phase takes place, essentially, at fixed chemical potential. This is the behavior expected for phase transitions in fluids, but not necessarily in gels (see below). The peculiarities of phase transitions in gels has been discussed by several authors.[33−38] Volume transitions taking place at constant surfactant concentration has been reported by others,[39] but discussed without reference to phase coexistence.

For the sample with $\beta = 0.15$, phase coexistence could not be ascertained. In this case, a surface phase (if present) is expected to be very thin and, therefore, difficult to detect. As will be discussed below, it may also contain large amounts of water and, therefore, be difficult to distinguish from the core. Even in the absence of a surface phase, the majority of the surfactant molecules in the gel would have formed micelles, as evident from a previous study,[14] where it was shown that micelles begin to form at $\beta \approx 0.01$.

The gels with $\beta > 0.8$ were homogeneous, i.e., no core could be observed, and had reached a contracted state beyond which an increase in the surfactant concentration in the solution did not result in any further deswelling. In this state, $V/V_0 = 0.04$, corresponding to a volume per polyion charge equal to 6×10^{-4} m^3/mol. The latter value is in agreement with earlier data for PA/C_{12}TAB in the absence of added NaBr,[14] where the volume per charge in fully collapsed gels was found to be $5-6 \times 10^{-4}$ m^3/mol, independent of the degree of cross-linking. Importantly, no further binding takes place after β has reached 0.9. This is also in agreement with data for the salt-free systems. In contrast, for the related system PA/C_{16}TAB, β was found to be ≥ 1 in the fully collapsed state.[16,17] For PA/C_{16}TAC, the complexes in the surface phase were found to have a 1:1 charge stoichiometry even at small β. Despite these differences, the reason for which is not clear, the volume per polyion charge in the fully collapsed gels is about the same for all systems.

We conclude from this section that the free concentration of surfactant in equilibrium with the surface phase of a partially collapsed gel is ca. 0.36 mM, the same concentration as needed to induce a volume collapse of a gel in a bulk surfactant solution. This result is important for the kinetic analysis in coming sections.

4.3. Swelling Isotherm. In Figure 8, we have combined the data from Figures 6 and 7 to obtain a swelling isotherm, showing how V/V_0 depends on β. The curve resembles the ones reported earlier for PA/C_{16}TAB and PA/C_{16}TAC,[17] and for PA/C_{12}TAB in the absence of salt,[14] but has a more pronounced sigmoid shape. The dashed line in Figure 8 is a theoretical swelling isotherm calculated from eqs 1− 3, 15, and 16, assuming that the surface phase has a fixed composition equal to that of the fully collapsed gel, i.e., $\upsilon_{skin} = 6 \times 10^{-4}$ m^3/mol, and a mole ratio of surfactant-to-polyion in the surface phase equal to 0.9, so that $\beta' = \beta/0.9$ for all β. To make the curve fit to the data at high β, where υ_{skin} and β' are known, $p = 80$ was selected. As can be seen, the calculated curve overestimates the effect caused by the surface phase, in particular at low β. In a previous paper[17] on PA/C_{16}TAC, it was demonstrated that the sigmoid shape of experimental curves could be reproduced by using as input in the calculations an experimentally determined relation between υ_{skin} and β, revealing that the water content of the surface phase decreased with increasing β. No such relationship has been determined for the present gels. Instead, we have fitted the model to the experimental data by adjusting υ_{skin} for each point. This procedure serves two purposes. First, we obtain V/V_0 as a continuous function of β that can be used as an empirical relationship when testing the kinetic model. Second, we obtain data showing how υ_{skin} depends on β, according to the model. The result, represented by the curve in Figure 9 and the solid line in Figure 8, suggests that υ_{skin} varies substantially, starting

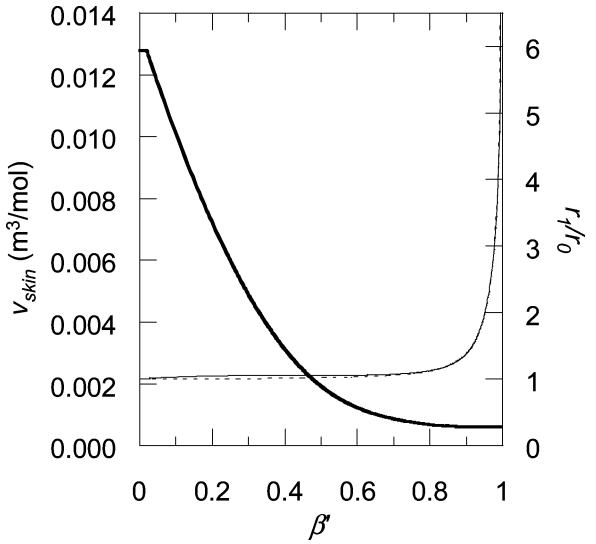

Figure 9. On the left axis (thick line) is shown υ_{skin} against β, illustrating that the surface phase initially is markedly more swollen than during the final stages of deswelling. On the right axis is the relative radius of the gel with surface phase (r_1) to the gel core (r_0), showing that even though the surface phase is more swollen at low β, the surface phase thickness is still negligible until $\beta > 0.8$. Further, r_1/r_0 is shown both with constant and variable υ_{skin} to illustrate the minor effect on surface phase thickness that using a variable υ_{skin} entails.

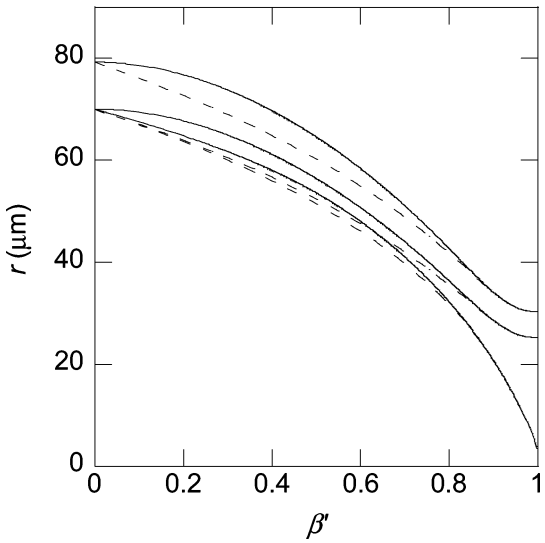

Figure 10. The radius of the core (r_0, lowest line), core + surface phase (r_1, middle line), and core + surface phase + stagnant layer ($r_1 + d$, upper line) at different β for a gel with $R_0 = 70$ μm in an average flow (υ) of 0.018 m/s. Solid lines represent a variable υ_{skin} (data from Figure 12), dotted lines a constant $\upsilon_{skin} = 6.04 \times 10^{-4}$ m^3/mol.

from a value close to υ_0, the volume per polyion charge in the surfactant free gel, to end at the value for the fully collapsed gels. While υ_{skin} at high β is essentially the same as that reported for PA/C_{16}TAC, it is 2−3 times larger at low β, indicating that there are substantial amounts of water in the surface phase. This is supported by the stickiness of the skins formed with C_{12}TAB; with C_{16}TAB/C_{16}TAC, they are more rubber-like.

A variation of υ_{skin} as indicated by Figure 9 provides the following explanation of the sigmoidality of the swelling isotherms: At a given lateral extension, a higher υ_{skin} corresponds to a lower compression of the surface phase network in the radial direction. Therefore, as the surface phase is less deformed, it imposes a smaller pressure on the core.[11,17] In addition to that, the contribution to the gel volume from the surface phase itself increases with increasing υ_{skin}, and so a transformation of part of the gel from core to surface phase can take place without noticeable volume reduction. Of course, these *in model* explanations may not be the whole truth. For instance, the sigmoidality may arise from strain softening, a well-known property of many networks[29] not accounted for by the theory behind eq 3.

We conclude that the equilibrium gel volume is determined by a complicated interplay between core swelling and surface phase contraction. The analysis provides relationships between the gel dimensions (r_0, r_1) and the amount of absorbed surfactant (β), essential for the rest of the paper. The geometrical basis for the theoretical description of the mass transport is exemplified in Figure 10 for a gel with $R_0 = 70$ μm ($\upsilon = 0.018$ m/s). Figure 9 shows the radius of the gel relative to the radius of the core (r_1/r_0) plotted against β', calculated both with a constant and a variable υ_{skin}, illustrating that the variation of υ_{skin} has only a small effect.

4.4. Choice of Conditions for Kinetic Experiments. The key assumption made in the kinetic model is that the response of the gel to a change in β is fast compared to the ion-exchange process (i.e., the binding of surfactant). Hence, the equilibrium-swelling isotherm is assumed to provide the correct relationship between V/V_0 and β also at intermediate stages during deswelling in a time-resolved experiment. The assumption cannot be tested directly because we cannot monitor the rate of binding to a single microgel; β can only be followed indirectly via the variation of V. We have found no means to determine equilibrium swelling isotherms for *single* microgels. Therefore, in the following test of the kinetic model, we will compare experimental deswelling curves with theoretical curves calculated from the swelling isotherm in Figure 8. The procedure is justified by the fact that the present microgels are macroscopic systems in a thermodynamic sense.

We have chosen to study gels primarily in the range $R_0 = 50-100$ μm, allowing accurate quantifications of gel radius. The surfactant concentration has been chosen so that the concentration difference (C_2 − cac) gives a deswelling period long enough to be easily recorded, but also short enough to ensure constant conditions during an experiment. All experiments have been performed in the presence of a swamping electrolyte (10 mM NaBr) so that the variations of the surfactant concentration have given only negligibly small changes to the osmotic pressure of the solution. Figure 11 shows *Sh* and *d*, the stagnant layer thickness, as functions of υ calculated from eqs A5 and A6a−c with $R_0 = 70$ μm (see figure legend for details). In the present study, $\upsilon \geq 0.018$ m/s, i.e., in a regime where variations should have only minor effects on the rate of mass transfer.

4.5. Kinetic Analysis. Images of a gel captured at different stages of deswelling are shown in Figure 12. A typical deswelling curve is shown in Figure 13, where the gel volume (V/V_0) is plotted vs time for a gel with radius $R_0 = 71$ μm. The volume of the gel in a flow ($\upsilon = 0.018$ m/s) of C_{12}TAB solution ($C = 0.61$mM) was measured as described in the Experimental Section. V_0 is the volume of the gel in 10 mM NaBr in the absence of surfactant. Note that V/V_0 is initially constant, followed by a steep deswelling curve that flattens out toward the end. The contributions to the lag time will be discussed separately in Section 4.7. Here, we focus on the deswelling kinetics. It should be stated, however, that all theoretical shrinking curves presented below have been adjusted horizontally so that $t = 0$ in the model coincides with the observed onset of deswelling. This was necessary due to large uncertainties in the calculation of lag times.

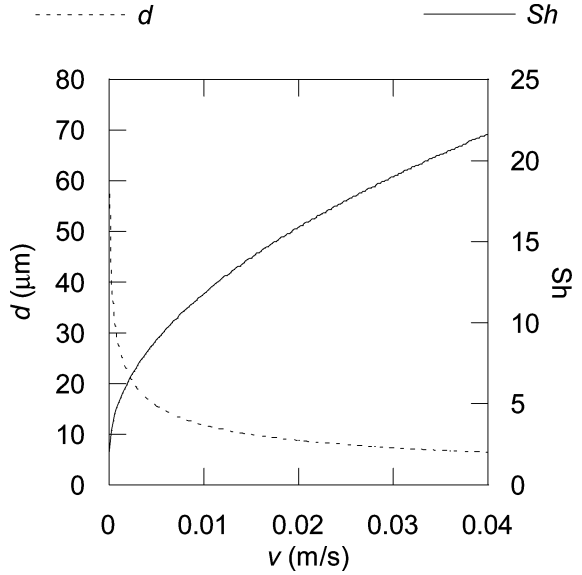

Figure 11. The influence of the liquid flow rate (v) on the Sherwood number *Sh* (right axis, solid line) and the stagnant layer thickness d (left axis, dotted line) for a gel with $R_0 = 70$ μm.

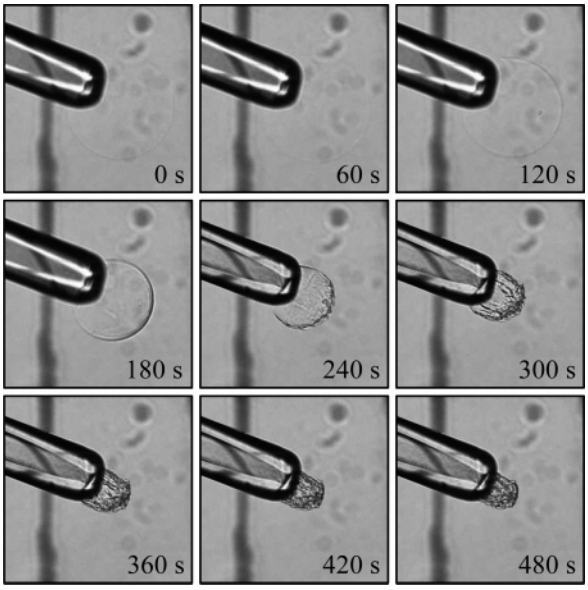

Figure 12. A gel held by the micromanipulator, deswelling in a flow of 0.56 mM C_{12}TAB, $v = 0.018$ m/s, for a total time of 480 s.

The solid line is a fit of the deswelling model to the experimental data using v_0, the volume per polyion charge in the fully swollen state, as a fitting parameter. All other inputs (except P) were taken from independent sources: the relationship between V/V_0 and β was taken from Figure 8, cac = 0.36 mM was determined from Figure 6, and $D = 4 \times 10^{-10}$ m^2/s was obtained from NMR self-diffusion measurements.[40] P was put equal to D. In Section 4.8, we show that this choice is in agreement with experimental diffusion data and also that it means that the theoretical curves are dominated by stagnant layer diffusion control. In fact, under the present conditions, the theoretical deswelling curves are very little affected by the value assigned to P as long as $P \geq$ D, as expected from the small thickness of the surface phase compared to the stagnant layer (Figure 10).

From the fit of the model, we obtain $v_0 = 0.026$ m^3/mol. This value is in good agreement with a previous estimate (0.022 m^3/mol) for PA gels made with the same concentration of cross-linker present. However, for the gels studied in Section 4.1, v_0 was found to be 0.013 m^3/mol. The reason for the discrepancy is not clear, but is probably related to the efficiency of incorporation of the cross-linker during gel synthesis. It should be pointed out that swelling isotherms, when normalized by V_0, were earlier found not to change much with the degree of cross-linking in the range from 1 to 3 mol % cross-linker,[14] in agreement also with model calculations.[17] Therefore, applying the swelling isotherm obtained in Section 4.1 to the microgels should introduce only minor errors.

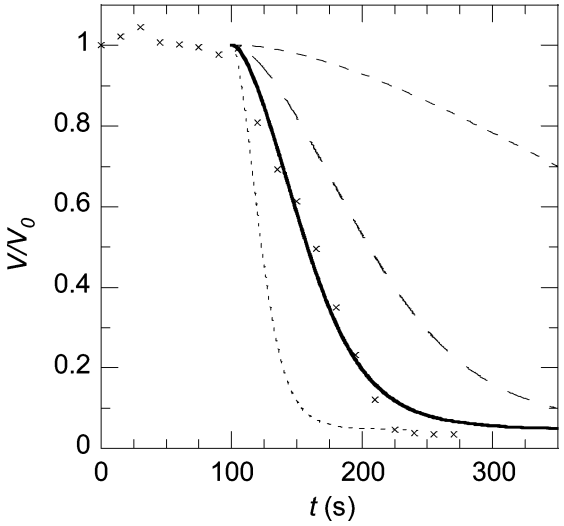

Figure 13. Example curve. Relative gel volume over time (theoretical and experimental) for a gel with $R_0 = 71$ μm in a 0.61 mM C_{12}TAB, 10 mM NaBr, pH 10 solution. $t = 0$ is set at the onset of deswelling. Shown are experimental crosses and the corresponding theoretical line (thick, solid). To illustrate how the deswelling profile changes with the different parameters, theoretical curves for the same gel in 0.4 mM (short, broken) and 1.0 mM C_{12}TAB (dotted) and a larger gel ($R_0 =$ 100 μm) in 0.61 mM (long, broken) are also included.

To illustrate the sensitivity of the model to different parameters, three additional theoretical lines are plotted in Figure 13: one each for the same gel in 0.4 and 1.0 mM C_{12}TAB, respectively, and one line for a larger gel ($R_0 = 100$ μm) in 0.61 mM. As evident, even a modest change in the parameters gives a rather large effect on the deswelling rate.

The strong dependence on R_0 is chiefly an effect of the ion-exchange reaction as such because the ratio v_0 / R_0^3 is proportional to the number of moles of polyion groups in a gel. It is also clear that a test of the model's predictive capacity would be meaningless if v_0 were to be used as a fitting parameter. Therefore, we will use $v_0 = 0.026$ m^3/mol for all microgels investigated. While this is expected to introduce errors due to variations between beads, the overwhelming advantage is that all theoretical curves will be direct model predictions obtained without parameter fitting.

4.6. Test of Kinetic Model. Experimental deswelling curves for gels in solutions containing 0.56, 0.61, 0.82, and 1.01 mM surfactant, respectively, can be found in Figures 14−17. The lines represent the theoretical curves calculated from the model. Considering that no fitting parameters are used, the agreement between theory and experiments is rather satisfactory. Most importantly, the variation of the deswelling rate with surfactant concentration is well described by the model, providing strong evidence that the kinetics are controlled by surfactant ion diffusion. Indeed, a higher bulk concentration gives a higher concentration difference (C_2 − cac) driving the influx of surfactant, resulting in shorter deswelling times.

One should be aware that the main problem when comparing the different concentrations is that it is nearly impossible to keep

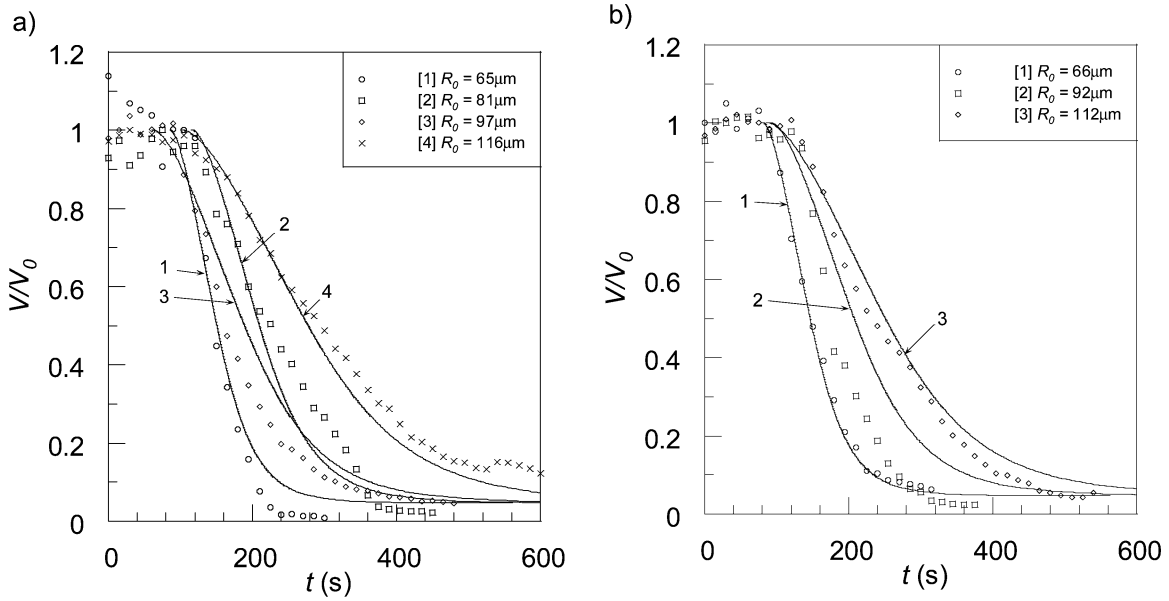

Figure 14. Deswelling kinetics for gels in 0.56 mM C_{12}TAB. Relative volume as a function of time for seven different sized gels, with corresponding theoretical lines, are shown. The data have been split into two graphs in order to facilitate easy reading.

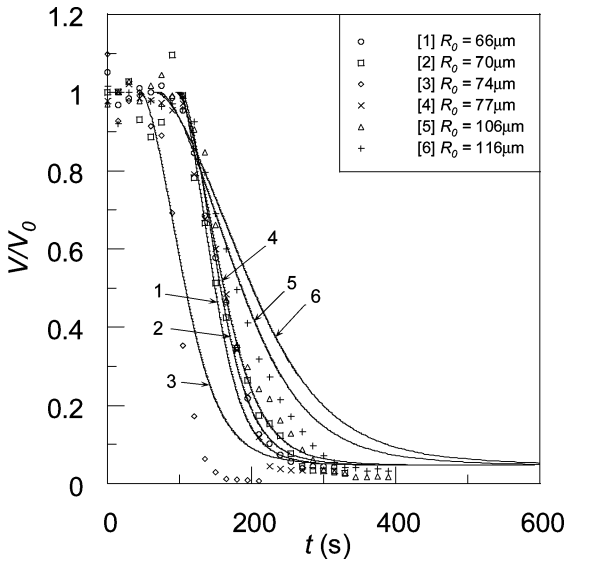

Figure 15. Deswelling kinetics for gels in 0.61 mM C_{12}TAB. Relative volume as a function of time for six different sized gels, with corresponding theoretical lines, are shown.

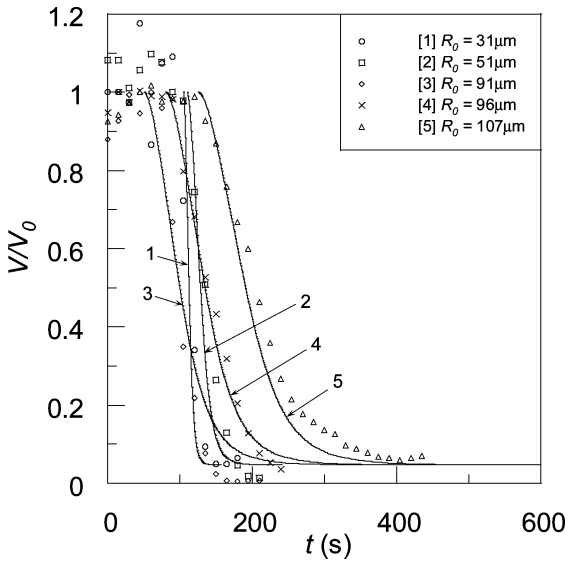

Figure 16. Deswelling kinetics for gels in 0.82 mM C_{12}TAB. Relative volume as a function of time for five different sized gels, with corresponding theoretical lines, are shown.

the gel radius (R_0) constant, as two gels never have exactly the same size, which results in more than one parameter being varied at the same time. This is further complicated by the fact that, because the Sherwood number (*Sh*) increases with gel radius, the stagnant layer, and thereby the total diffusion path and the deswelling time, will increase even more than the gel radius, making the gel size relatively more influential than the other parameters. However, because the theoretical model takes into account the dependence of both the surfactant concentration and the gel radius, the main difficulty lies in the illustration and comparison of the results, as the different gels used will have slightly different theoretical deswelling times even at the same surfactant concentration.

As mentioned above, the gel size is naturally varied, but care was also taken to intentionally test gel sizes over a larger interval with all other parameters constant. This can be seen perhaps most clearly for 0.82 mM C_{12}TAB in Figure 16, where the gel radius is $31 < R_0 < 106$ μm. Note that the larger gels have markedly longer deswelling times and also that the theory is able to account for the variations, favoring the explanation of stagnant layer diffusion as the rate controlling process under the conditions studied here.

The third parameter to be varied was the flow rate, which normally was set to 0.018 m/s. Figure 18 shows the results for gels in 0.82 mM C_{12}TAB at a flow rate of 0.027 m/s. These should be compared to the curves in Figure 16, with consideration taken to the different gel sizes, as those gels are in the same surfactant concentration but at a normal flow rate. Note that the gels in a higher flow have shorter deswelling times. The variation is accounted for quantitatively by the model, again indicating that mass transport in the liquid surrounding the gels has a strong influence on the kinetics, and that the stagnant layer approximation can be used to describe it.

No attempts were made to test quantitatively the model at lower flow rates due to large uncertainties in the estimation of the Sherwood number in this range, as shown by Figure 11.

4.7. Lag Time. According to the model (assumptions 1, 2), deswelling starts when the ion exchange between sodium ions

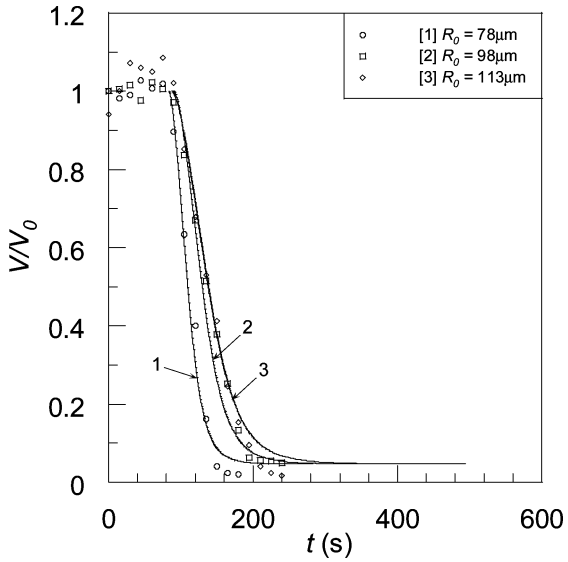

Figure 17. Deswelling kinetics for gels in 1.01 mM C_{12}TAB. Relative volume as a function of time for three different sized gels, with corresponding theoretical lines, are shown.

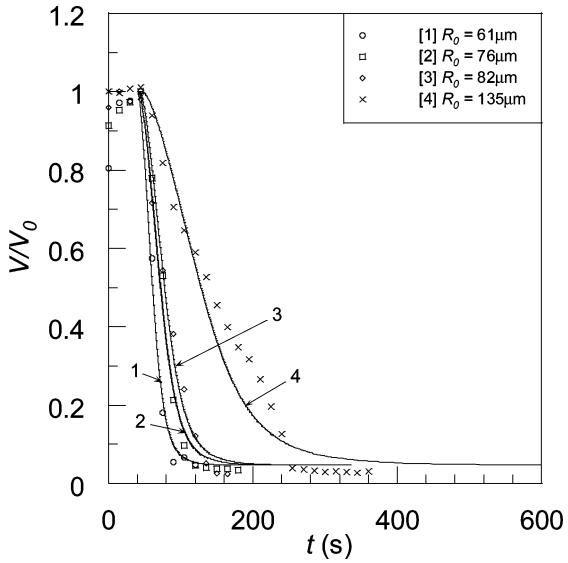

Figure 18. Deswelling kinetics for gels in 0.82 mM C_{12}TAB at a higher flow rate (0.027 m/s). Relative volume as a function of time for four different sized gels, with corresponding theoretical lines, are shown.

and surfactant ions has proceeded to the extent that the average surfactant concentration in the gel reaches the critical aggregation concentration. To test this, we have calculated theoretical lag times for the data in Figures 13−18 by using equations available in the literature on ion exchange.[30] Please note that the time given on the abscissa in theses plots includes the time required for the surfactant solution to travel from the reservoir to the flow pipet where the gel is positioned. The latter is 71 s for the flow rate used in Figures 13−17, and 40 s in Figure 18, as determined in separate experiments. As can be seen, this is the largest contribution to the time delay before deswelling starts. Two limiting cases have been considered: particle diffusion control and stagnant layer (film) diffusion control.[30] (A detailed description of the application of the equations to the present system are given elsewhere.[10]) In both cases, the lag time increases with increasing gel size, decreasing surfactant concentration in the solution (smaller thermodynamic driving force), and in the case of film diffusion control, with decreasing liquid flow rate. The calculation shows that, for the present systems, the two models give lag times of the same order of magnitude. For example, the lag time for the beads in Figure 16 (0.56 mM) increases from 3 to 9 s according to particle diffusion control, and from 5 to 13 s according to film diffusion control, going from the smallest to the largest radius. In Figure 17 (1.01 mM), the corresponding results are 0.8−2 s and 2−4 s, respectively. In the calculations, we have assumed that the diffusion constant inside a bead is 0.76 times that in the solution due to the interactions with the polyion charges. The reduction factor was reported for C_8TAB in 50 mM solutions of linear sodium polyacrylate.[41] The calculations indicate that the kinetics is in a range intermediate between particle and film diffusion control, for which case there is no rigorous analytical solution available.[30] However, from simple reasoning, it is clear that, under these conditions, the concentration gradient inside a bead, at a given time, must be, on the average, flatter than that for particle diffusion control. The same can be said about the gradient outside the bead. Therefore, the total lag time must be somewhat larger than the sum of particle and film diffusion control (i.e., 8−22 s and 3−6 s, respectively). According to Figure 14, the lag time at 0.56 mM surfactant increases from 10 to 40 s, going from the smallest to the largest bead. At 1.01 mM, it is about 20 s (Figure 17). The lag times are slightly larger than the sum of the theoretical lag times for particle and film diffusion control, but not larger than expected when both particle and film diffusion influence the ion-exchange rate. Therefore, we conclude that assumptions 1 and 2 in the model are not in conflict with the observed lag times and thus that there appear to be no important free energy barrier associated with the onset of deswelling. The poor quality of the data during the lag period in some of the experiments is due to low contrast, making it difficult to focus on the rim of the bead. During deswelling, this was not a problem because the surface phase provided contrast. Before ending this section, it should be pointed out that diffusion in the core is not expected to affect the deswelling rate despite its influence during the lag period. The reason for this is that during the deswelling process, the core is "saturated" with surfactant monomers, and so the surfactant needs only to diffuse through the surface phase for deswelling to proceed.

4.8. Transport Through the Surface Phase. So far, we have compared experimental data with theoretical calculations based on eq 5 with $P = D$. Equation 9 offers a way to calculate the deswelling rate directly from the diffusion constant in the surface phase without having to make assumptions about the magnitude of P. Unfortunately, no experimental determination of D_I has been made for $C_{12}TA^+$ in the surface phase. However, there are NMR data available for two related systems in the literature. One is from the micellar cubic phase (space group: $Pm3n$) in the C_{12}TAC/water system (ca. 50 wt % water), where the surfactant self-diffusion coefficient was found to be 5×10^{-13} m^2/s.[42] The other is from the micellar cubic phase ($Pm3n$) formed by the complex salt C_{16}TA/(linear)PA in water, where the diffusion coefficient for $C_{16}TA^+$ was found to be 1×10^{-14} m^2/s.[43] Importantly, the latter was nearly constant, even when the composition of the cubic phase was gradually changed by replacing the polyion for acetate ions at a fixed water content of 50 wt %.[43] The result shows that the nature of the counterion, monovalent or polyvalent, does not influence the diffusion coefficient in the system. Therefore, because the phase structure for the collapsed phases formed in the present system strongly resembles the one in the C_{12}TAC/water cubic phase (same space group[18]), one expects D_I to be close to 5×10^{-13} m^2/s. Further support comes from theoretical considerations of the diffusion process. In a cubic phase, where the micelles are stationary, a

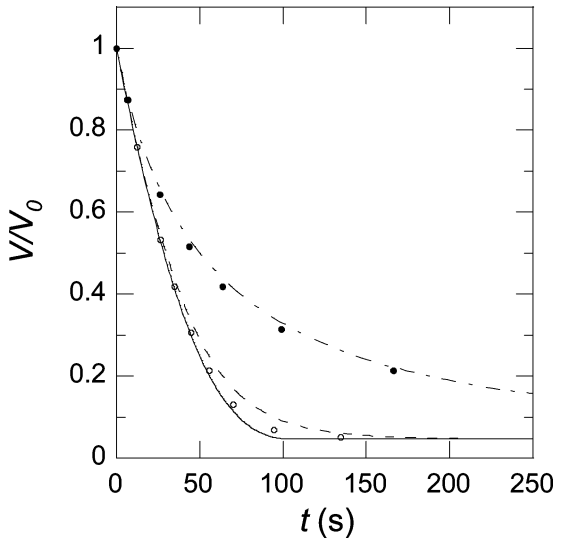

Figure 19. Theoretical deswelling curves calculated from eqs 9 and 14 with D_I equal to 5×10^{-13} m^2/s (open symbols) and 1×10^{-14} m^2/s (filled symbols), and from eq 5 with $D/P = 0$ (solid line), $P = 4 \times 10^{-10}$ m^2/s (dashed line), and $P = 4.2 \times 10^{-11}$ m^2/s (dashed−dotted line). Common to all curves: $D = 4 \times 10^{-10}$ m^2/s, $C_2 = 1$ mM, cac = 0.36 mM, $C = 1.5$ M, $R_0 = 70$ μm, $\upsilon_{skin} = 6.04 \times 10^{-4}$ m^3/mol, and $\upsilon = 0.018$ m/s.

rough estimate of the diffusion coefficient is obtained by taking the fraction of surfactant in the aqueous region between the micelles times the self-diffusion coefficient in water.[43] An estimate of the average monomer concentration in the water in the C_{12}TAC cubic phase can be obtained from the Poisson−Boltzmann cell model.[44] The calculations were made for spherical micelles at a total concentration of 1.9 M (50 wt %), as described in detail elsewhere.[45] The result is 0.6 mM, which gives a diffusion coefficient of 2×10^{-13} m^2/s, in reasonable agreement with experiments. Now, because the monomer concentration is close to the cac in the present system, the diffusion coefficient should also be about the same. Note that the low diffusion coefficient reported for $C_{16}TA^+$ is consistent with the fact that it has small cmc and cac values.

Figure 19 shows the deswelling according to eqs 9 and 11 with $D_I = 5 \times 10^{-13}$ m^2/s, cac = 0.36 mM, $C_2 = 1$ mM, and $C = 1.5$ M (open symbols). The dimensions of the system at any stage are the same as in Figure 10. The value of C corresponds to the composition of gels in the fully collapsed state in Figure 8. It can be extracted out from the calculations (not shown) that C_1 is close to cac during the major part of the binding (but starts to increase rapidly for $\beta > 0.7$), showing that stagnant layer diffusion dominates. For comparison, curves are shown resulting from eq 5 for the case of complete stagnant layer diffusion control ($D/P = 0$) (solid line), and $P = D$ (dashed). In as much as eq 9 is reliable, the following conclusions can be made: (1) the transport through the surface phase does not influence the kinetics to any appreciable extent as long as D_I is on the order of 5×10^{-13} m^2/s, and (2) eq 5 with $P = D$ gives a good description, except at large β, where the surface phase is thick (see Figure 10).

To investigate the case of slow transport in the surface phase, we have included in Figure 19 the result from a calculation by using eq 9 with $D_I = 1 \times 10^{-14}$ m^2/s (filled symbols); all other parameters are the same as before. It is evident from the slow relaxation rate that the surface phase has a large influence. It can be extracted out that C_1 increases rapidly from 0.36 mM at $\beta \approx 0$ ($t \approx 0$) to the bulk value during the course of binding. According to eq 14, P then decreases from 4.2×10^{-11} to 2.4×10^{-11} m^2/s, highlighting the problems with this quantity. However, if P reaches the lower value fast enough, eq 5 is expected to give a reasonable description. The dash−dotted line in Figure 19, valid for $P = 2.4 \times 10^{-11}$ m^2/s and $C_1 = C_2 = 1$ mM (i.e., no influence from the stagnant layer), illustrates that this is the case here.

Interestingly, a low diffusion constant does not necessarily imply slow transport through the surface phase because a low cac compensates for this by giving rise to a large difference in chemical potential, speeding up the process. For instance, by using eq 14 to calculate the permeability for $C_{16}TA^+$ for a surface phase in contact with a 1 mM solution of the surfactant (10 mM NaBr), one obtains $P = 9 \times 10^{-11}$ m^2/s ($D_I = 1 \times 10^{-14}$ m^2/s; cac $= 2 \times 10^{-6}$ M;[46] $C = 1.5$ M[17]). This value would give only small deviations from stagnant-layer-controlled kinetics. The result has interesting implications to the binding/release of proteins to/from gels, where diffusion constants can be very small. Thus, a large binding constant, leading to a very low C_0 (equal to cac in the analysis above), will promote a rapid transport through the surface phase.

It should be mentioned that, very recently, Kabanov and coworkers[9] proposed a mechanism for the binding of proteins to oppositely charged macrogels, described as a "frontal relay race propagating a heterogeneous reaction". The same mechanism had earlier been proposed for the binding of linear polyions and surfactants.[13,47] In their model, the rate of binding is controlled by the formation of "vacancies" at the boundary between the core and the surface phase due to thermal fluctuations *if* it equals the rate of transport of the vacancies from the core boundary to the gel surface, where the latter rate depends on counterion diffusion through the surface phase (see Section 4.9). However, the result of their mathematical analysis, which is not based on Fickian diffusion, depends on a first-order rate constant of protein uptake. We prefer to describe the process as a diffusion of surfactant. No matter what the mechanism for transport is, this is always possible as long as there is a well-defined difference in chemical potential over the surface phase.

4.9. Sodium Ion Diffusion. As mentioned earlier, the diffusion coefficient D used in the calculations should be an effective diffusion coefficient for C_{12}TAB. The reason for this can be found by looking closer at the factors determining the formation of new micelles and the subsequent phase transition. To form new micelles, $C_{12}TA^+$ monomers must diffuse through the stagnant layer and the surface phase and into the core. For each monomer that diffuses into the core, a Na^+ ion must diffuse out from the gel to maintain electroneutrality (neglecting the amount of bromide ions entering the surface phase). The D governing the diffusion should, therefore, be an average interdiffusion coefficient for Na^+ and $C_{12}TA^+$. It is known from the theory of ion exchange that the ion present in smaller concentration has the stronger effect on the rate of interdiffusion.[30] Conveniently, in the stagnant layer, where $[Na^+] \gg [C_{12}TA^+]$, the interdiffusion coefficient should be very close to the $C_{12}TA^+$ self-diffusion coefficient, as we have assumed here. For the surface phase, where we do not know the concentration of sodium ions, the situation is less obvious. However, because of the large excess of sodium ions in the solution in contact with the gel, the aqueous regions between micelles in the surface phase is likewise expected to contain an excess of sodium ions over surfactant monomers.

4.10. Relation Between cac and Volume Transition. In the literature, cac is usually defined as the total surfactant concentration in a polymer solution where micelles can first be detected.

For the binding to gels, we have defined cac as the concentration or, more precisely, the activity, in the solution at the point where micelles can be detected in the gel.[14] In the kinetic equations, we have used cac to denote the surfactant activity at the boundary between the core and the surface phase. The local concentration of unimers in the core is different from cac because of the Donnan effect (nonuniform distribution of ions between a charged gel and a solution), but at equilibrium, the activity equals that in the solution. In principle, the surfactant activity in the core need not necessarily be constant when the degree of swelling of the network is changed. However, because the binding isotherm shows that the free concentration (activity) of surfactant is equal to cac at least up until $\beta = 0.8$, that would only result in a slight alteration of the tails of the deswelling curves.

Another issue that deserves some clarification is the relation between cac and volume change. The problem is relevant because $C_1 =$ cac is used as a boundary condition in the kinetic analysis. For comparison, we have included in Figure 7 binding data for C_{12}TAB in solutions of 0.5 mM linear PA and 10 mM NaBr, reported earlier.[48] The data were obtained at surfactant concentrations below the phase separation limit.[41] According to the binding isotherm, cac = 0.31 mM. In the excess of added salt, the binding to the polyion at concentrations below the cac can be neglected.[49] Therefore, cac is equal to the free concentration at the onset of cooperative binding. From considerations based on the magnitude of the cac, and other observations (see ref 48 for a summary), it has been established that $C_{12}TA^+$ micelles formed in PA solutions (at the cac) are decorated with a layer of the polyion and that this arrangement is essential for their existence. Therefore, the presence of micelles always reduces the average size of the PA coils. In solutions, this can be the result of single micelles interacting independently with part of a polyion chain, or several micelles collectively binding to one or several chains. Thus, polyion contraction should always coincide with the cac. In gels, the effect produced by each micelle is transferred to all chains in the network and is therefore expected to give rise to a volume change. The data in Figure 7 show that cooperative binding starts at the same concentration in solutions and in gels. Thus, one expects the deswelling to start at the cac. At sufficiently low concentrations, $C_{12}TA^+$ monomers bind to the gel through a simple ion-exchange reaction.[14] Above cac, the binding is cooperative, and micelles can be detected in the gel.[14] Because of the elastic energy stored in the network, deswelling is expected to coincide with cooperative binding because the swelling pressure is reduced when micelles replace sodium ions.[50] However, the onset of deswelling has been found to start at a somewhat higher concentration.[14] Because of heterogeneity and defects in the network, there may be sites in a gel where micelles can form without leading to a measurable deswelling. Therefore, cac and the onset of deswelling do not necessarily coincide. Fortunately, the evaluation of the kinetic model is little affected by these complications of two reasons: First, we use an empirical relation between gel volume and β. Second, the binding isotherm shows that the cac used in the model represents, in fact, the activity of the surfactant in equilibrium with the surface phase for the major part of the deswelling.

4.11. Kinetics of Swelling. As has been shown above, the uptake of surfactant and subsequent deswelling of polyacrylate gels seems to be controlled by stagnant layer diffusion. One can then pose the question whether the release of surfactant from a collapsed gel is also governed by stagnant layer diffusion. For the present system, we have observed that, when a collapsed gel is placed in a solution with $C <$ cac, the polyelectrolyte/micelle complexes will start to dissolve and the gel will swell. This process takes place from the outside and inward, so that a collapsed core is surrounded by a swollen outer part. This means that the process will principally be the same as for deswelling, but with two major differences: First, that the distance the surfactant needs to diffuse will for the most part be longer, as it will be through swollen gel instead of the collapsed surface phase (the exception being the very first stage of swelling). Second, that the concentration difference driving the diffusion will at the most be between cac (0.36 mM) and zero, instead of between cac and a high concentration (0.47−1.0 mM in our experiments). This will give a difference of $\Delta C \leq 0.36$ mM instead of $\Delta C = 0.11-0.77$ mM.

Altogether, this means that the release of surfactant for most cases is likely to be slower than the uptake measured here, making ion-exchange kinetics and stagnant layer diffusion during release equally or even more important.

5. Conclusions

The surfactant-induced volume transition of oppositely charged microgels is a complex process involving a dynamic interplay of ion exchange, mass transport, network contraction, surfactant self-assembly, and phase separation. In this paper, we argue that there are two circumstances simplifying the kinetics to such an extent that even quantitative predictions of deswelling rates can be made for a range of experimental conditions. The first is that rate of volume change is controlled by the rate of surfactant binding to the gel core, and the second is that the equilibrium-swelling isotherm applies also at intermediate stages during the volume transition. We have shown that a mathematical model derived earlier,[10] valid under those circumstances, accounts for the shape of the experimental deswelling curves and the dependences of the deswelling rate on variations in liquid flow rate, surfactant concentrations, and gel size. In as much as the good agreement with the experiments proves that the model is correct, the most important features of the volume transition are the following: During the transition, the gel is in a phase separated state.[10] The volume of the gel decreases as the swollen core is gradually converted into collapsed surface phase. An ion-exchange process governs the growth of the surface phase, where sodium ions in the core are replaced by surfactant ions forming micelles at the interface between the core and the surface phase. As long as the thickness of the surface phase is small, the rate-controlling step in this process is the mutual transport of surfactant ions to, and sodium ions from, the gel surface. In the excess of sodium ions in the solution, this is controlled by the transport of surfactant in the liquid layers surrounding the gel, satisfactorily described using dimensionless numbers. In comparison, the relaxation processes within the gel, i.e., transport of material through the surface phase, and rearrangements of material (network, micelles), is fast. Osmotic pressure differences between the gel core and the electrolyte solution are, therefore, quickly evened out, and so the gel volume is the same as it would be at equilibrium with the same amount of bound surfactant. In contrast, by changing the experimental conditions, a setup could be found in which surface phase permeability, transport through the surface phase, and/or network relaxation become rate controlling. Such experiments will be conducted soon.

The surface phase simplifies the description of the ion-exchange kinetics by fixing the activity of the surfactant at the core interface. The uncoupling of the kinetics and the gel swelling is a useful approximation for the present system, greatly simplifying the kinetic analysis.

The equilibrium properties of the PA-gel/C_{12}TAB system reported here are in agreement with the general picture established earlier and observed for related systems.[13,17] A volume transition from a surfactant-free swollen state to a collapsed surfactant-rich state takes place in a narrow range of surfactant concentrations in the equilibrium aqueous phase. At intermediate amounts of absorbed surfactant, a collapsed surface phase is formed, enclosing the swollen core network. However, the swelling isotherm (V/V_0 vs β) has a more pronounced sigmoid shape than that reported for other systems in the literature. The reason for this is not clear, but an analysis using the equilibrium swelling model derived earlier[17] indicates that the water content in the surface phase may decrease gradually with increasing β, contributing to the observed effect. More structural and compositional information about the surface phase is required to resolve this.

The experiments described in this paper demonstrate that single microgel beads are conveniently studied in a microscope while positioned in a controlled liquid flow using a micropipet. For future applications of the technique, a means to determine the amount of substance absorbed/released by a single microgel would be useful. In general, the reproducibility of an experiment is hampered, not only by variations in gel size, but also by variations in composition. The problem can be solved, when possible, by doing repeated experiments with one gel bead.[11]

Finally, our results suggest that volume transitions coupled to ion-exchange processes in gels of the present size range or smaller, should always be strongly influenced by stagnant layer diffusion. This is of relevance for understanding, e.g., the release kinetics in drug delivery systems based on gels, and for the rate of secretion of substances from secretory vesicles, an important topic in physiology.[1,51]

Acknowledgment. This work was supported by a grant from the Swedish Foundation for Strategic Research (SFF).

Appendix 1

Poission-Boltzman Cell Model.[44,52,53] The polyion is described as an infinitely long cylinder with radius $a = 2$ Å with a uniform surface charge density (σ) of $e/(2\pi ab)$, where b is the actual distance between charges on the polyion ($b = 2.5$ Å), and e is the charge of an electron. The cylinder is situated in the center of a cylindrical cell of radius $L + a$ (L being the water-layer thickness, which can be calculated from v_{core}) containing water and mobile ions. The mobile ion distribution in the cell can be obtained by solving the PB equation, which in cylindrical coordinates becomes

$$\frac{1}{r}\frac{\mathrm{d}}{\mathrm{d}r}\left(r\frac{\mathrm{d}\Phi}{\mathrm{d}r}\right) = -\frac{e}{\epsilon_0\epsilon_r}\sum_i z_i c_i \exp\left(\frac{-z_i e\Phi}{kT}\right) \qquad \text{(A1)}$$

where Φ is the electrostatic potential, ϵ_0 is the permittivity of vacuum, ϵ_r is the relative permittivity of water, z_i the valence of ion i, c_i is the bulk electrolyte concentration in moles/m^3, k the Boltzmann constant, and T the temperature in Kelvin. The equation is solved numerically with the constraints

$$(\mathrm{d}\Phi/\mathrm{d}r)_{r=L+a} = 0 \qquad \text{(A2a)}$$

$$(\mathrm{d}\Phi/\mathrm{d}r)_{r=a} = -\sigma/(\epsilon_0\epsilon_r) \qquad \text{(A2b)}$$

in our case by using a computer program written by Bengt Jönsson.[54]

According to the PB cell model, the osmotic pressure is equal to

$$\pi_{ion} = RT\sum_i C_i(L + a) \qquad \text{(A3)}$$

By neglecting ionic interactions in the solution, $\Delta\pi_{ion}$ can then be calculated as

$$\Delta\pi_{ion} = RT\sum_i C_i(L + a) - 2RTC_{salt} \qquad \text{(A4)}$$

for a range of values of v_{core}.

Appendix 2

Stagnant Layer Diffusion. The stagnant layer thickness d (Figure 11), a fictitious quantity constructed to simplify calculations of mass transfer, is defined as the ratio between D and the mass transfer coefficient,[24] and can be expressed as

$$d = \frac{2r_1}{Sh} \qquad \text{(A5)}$$

were Sh is the Sherwood number. Equation A5 is valid for single spheres. Under conditions of forced convection, Sh is a function of the Reynolds (Re) and Schmidt (Sc) numbers. For $Re < 20$:[24]

$$Sh \approx 2.0 + 0.6(Re)^{1/2}(Sc)^{1/3} \qquad \text{(A6a)}$$

$$Re = \frac{2vr_1\rho}{\eta} \qquad \text{(A6b)}$$

$$Sc = \frac{\eta}{\rho D} \qquad \text{(A6c)}$$

where v is the liquid velocity, ρ is the liquid density, and η is the liquid viscosity.

References and Notes

(1) Rahamimoff, R.; Fernandez, J. M. *Neuron* **1997**, *18*, 17.
(2) Burgess, T. L.; Kelly, R. B. *Annu. Rev. Cell Biol.* **1987**, *3*, 243.
(3) Arvan, P.; Castle, D. *Biochem. J.* **1998**, *332*, 593.
(4) Alberts, B.; Johnson, A.; Lewis, J.; Raff, M.; Roberts, K.; Walter, P. *Molecular Biology of the Cell*, 4th ed.; Garland Publishing: New York, 2002.
(5) Kiser, P. F.; Wilson, G.; Needham, D. *Nature* **1998**, *394*, 459
(6) Kiser, P. F.; Wilson, G.; Needham, D. *J. Controlled Release* **2000**, *68*, 9.
(7) Uvnäs, B.; Åborg, C.-H. *News Physiol. Sci.* **1989**, *4*, 68.
(8) Marszalek, P. E.; Farrell, B.; Verdugo, P.; Fernandez, J. M. *Biophys. J.* **1997**, *73*, 1169.
(9) Kabanov, V. A.; Skobeleva, V. B.; Rogacheva, V. B.; Zezin, A. B. *J. Phys. Chem. B* **2004**, *108*, 1485.
(10) Göransson, A.; Hansson, P. *J. Phys. Chem. B* **2003**, *107*, 9203.
(11) Andersson, M.; Råsmark, P. J.; Elvingson, C.; Hansson, P. *Langmuir* **2005**, *21*, 3773.
(12) Khokhlov, A. R.; Kramarenko, E. Y.; Makhaeva, E. E.; Starodubtzev, S. G. *Macromolecules* **1992**, *25*, 4779.
(13) Kabanov, V. A.; Zezin, A. B.; Rogacheva, V. B.; Khandurina, Y. V. *Macromol. Symp.* **1997**, *126*, 79.
(14) Hansson, P. *Langmuir* **1998**, *14*, 2269.
(15) Khandurina, Y. V.; Rogacheva, V. B.; Zezin, A. B.; Kabanov, V. A. *Polym. Sci.* **1994**, *36*, 184.
(16) Hansson, P.; Schneider, S.; Lindman, B. *Prog. Colloid Polym. Sci.* **2000**, *115*, 342.
(17) Hansson, P.; Schneider, S.; Lindman, B. *J. Phys. Chem. B* **2002**, *106*, 9777.
(18) Hansson, P. *Langmuir* **1998**, *14*, 4059.
(19) Svensson, A.; Piculell, L.; Karlsson, L.; Cabane, B.; Jönsson, B. *J. Phys. Chem. B* **2003**, *107*, 8119.
(20) Karabanova, V. B.; Rogacheva, V. B.; Zezin, A. B.; Kabanov, V. A. *Polym. Sci.* **1995**, *37*, 1138.

(21) Skobeleva, V. V.; Rogacheva, V. B.; Zezin, A. B.; Kabanov, V. A. *Dokl. Phys. Chem.* **1996**, *347*, 52.
(22) Skobeleva, V. B.; Zinchenko, A. V.; Rogacheva, V. B.; Zezin, A. B.; Kabanov, V. A. *Polym. Sci., Ser. A* **2001**, *43*, 315.
(23) Eichenbaum, G. M.; Kiser, P. F.; Simon, S. A.; Needham, D. *Macromolecules* **1998**, *31*, 5084.
(24) Coulson, J. M.; Richardson, J. F.; Blackhurst, J. R.; Harker, J. H. *Coulson & Richardson's Chemical Engineering*, 5th ed.; Butterworth-Heinemann: Oxford, 1996; Vol. 1.
(25) Maeda, T.; Ikeda, M.; Shibahara, M.; Haruta, T.; Satake, I. *Bull. Chem. Soc. Jpn.* **1981**, *54*, 94.
(26) Hayakawa, K.; Kwak, J. C. T. *J. Phys. Chem.* **1982**, *86*, 3866.
(27) Ricka, J.; Tanaka, T. *Macromolecules* **1984**, *17*, 2916.
(28) Treloar, L. R. G. *The Physics of Rubber Elasticity*; Oxford University Press: New York, 1958.
(29) Rubinstein, M.; Colby, R. H. *Polymer Physics*; Oxford University Press: New York, 2003.
(30) Helfferich, F. *Ion Exchange*; McGraw-Hill: New York, 1962.
(31) Evans, F.; Wennerström, H. *The Colloidal Domain: Where Physics, Chemistry, Biology, and Technology Meet*; VCH Publishers: New York, 1994.
(32) Fan, L. T.; Singh, S. K. *Controlled Release. A Quantitative Treatment*; Springer-Verlag: Berlin, 1989; Vol. 13.
(33) Hirotsu, S. *J. Chem. Phys.* **1987**, *88*, 427.
(34) Sekimoto, K.; Kawasaki, K. *Physica A* **1989**, *154*, 384.
(35) Sekimoto, K. *Phys. Rev. Lett.* **1993**, *70*, 4154.
(36) Tomari, T.; Doi, M. *Macromolecules* **1995**, *28*, 8334.
(37) Moerkerke, R.; Koningsveld, R.; Berghmans, H.; Dusek, K.; Solc, K. *Macromolecules* **1995**, *28*, 1103.
(38) Panyukov, S.; Rabin, Y. *Macromolecules* **1996**, *29*, 8530.
(39) Sasaki, S.; Koga, S.; Imabayashi, R.; Maeda, H. *J. Phys. Chem. B* **2001**, *105*, 5852.
(40) $D = 4.42 \times 10^{-10}$ m^2/s in D_2O at 298 K. Prof. Olle Söderman, unpublished data.
(41) Thalberg, K.; Lindman, B.; Bergfeldt, K. *Langmuir* **1991**, *7*, 2893.
(42) Bull, T.; Lindman, B. *Mol. Cryst. Liq. Cryst.* **1974**, *28*, 155.
(43) Svensson, A.; Topgaard, D.; Piculell, L.; Söderman, O. *J. Phys. Chem. B* **2003**, *107*, 13241.
(44) Gunnarsson, G.; Jönsson, B.; Wennerström, H. *J. Phys. Chem.* **1980**, *84*, 3114.
(45) Hansson, P.; Jönsson, B.; Ström, C.; Söderman, O. *J. Phys. Chem. B* **2000**, *104*, 3496.
(46) Hansson, P. Polyelectrolyte-Induced Assembly of Ionic Surfactants. Ph.D. Thesis, University of Uppsala, 1995.
(47) Zezin, A. B.; Rogacheva, V. B.; Kabanov, V. A. *Macromol. Symp.* **1997**, *126*, 123.
(48) Hansson, P.; Almgren, M. *J. Phys. Chem.* **1995**, *99*, 16684.
(49) Hansson, P. *Langmuir* **2001**, *17*, 4167.
(50) Khokhlov, A. R.; Kramarenko, E. Y.; Makhaeva, E. E.; Starodoubtzev, S. G. *Makromol. Chem., Theory Simul.* **1992**, *1*, 105.
(51) Verdugo, P. *Annu. Rev. Physiol.* **1990**, *54*, 157.
(52) Fuoss, R. M.; Katchalsky, A.; Lifson, S. *Proc. Natl. Acad. Sci. U.S.A.* **1951**, *37*, 579.
(53) Marcus, R. *J. Chem. Phys.* **1955**, *23*, 1057.
(54) Computer program written by Bengt Jönsson available at http://www.fkem2.lth.se/education/kursinfo/molvxv_dynamik/pbcell.exe.zip.